



Synthesis, in vitro and in vivo preliminary evaluation of anti-angiogenic properties of some pyrroloazaflavones

Maria Grazia Ferlin^{a,*}, Maria Teresa Conconi^a, Luca Urbani^a, Barbara Oselladore^b, Diego Guidolin^b, Rosa Di Liddo^a, Pier Paolo Parnigotto^a

^a Department of Pharmaceutical Sciences, University of Padova, via F. Marzolo, 5, 35131 Padova, Italy

^b Department of Human Anatomy and Physiology, University of Padova, Anatomy Section, via A. Gabelli, 65, 35131 Padova, Italy

ARTICLE INFO

Article history:

Received 21 April 2010

Revised 27 October 2010

Accepted 4 November 2010

Available online 10 November 2010

Keywords:

Pyrroloazaflavones

Phenyl-pyrroloquinolinones

Angiogenesis

Anti-vascular agents

ABSTRACT

This work investigated the in vitro and in vivo anti-angiogenic activity of some pyrroloazaflavones, exactly 2-phenyl-1*H*-pyrrolo[2,3-*h*]quinolin-4(7*H*)ones, with vinblastine as reference compound. Growth inhibitory activity, migration, and capillary-like structures formation were determined in human umbilical vein endothelial cell cultures, and Matrigel plug assay was carried out to evaluate in vivo effects on angiogenesis. Collectively, our results indicate that some pyrroloazaflavone derivatives, at non-cytotoxic concentrations and like vinblastine are able: (i) to exert in vitro anti-angiogenic activity and (ii) to counteract in vitro and in vivo the pro-angiogenic effects of fibroblast growth factor-2 (FGF-2).

© 2010 Elsevier Ltd. All rights reserved.

1. Introduction

In tumor pathogenesis, angiogenesis is crucial and it sustains malignant cells with nutrients and oxygen. Tumor cells secrete various growth factors which trigger endothelium cells to form new capillaries. Preventing the expansion of new blood vessel network results in reduced tumor size and metastases. Since angiogenesis is essential for tumor development and tumor vasculature is considered an optimal target for anti-cancer strategies, the research aimed at discovering anti-angiogenic agents as a treatment of malignancy or as an adjunct to standard chemotherapeutic regimens, is very active. The targeting of tumor vasculature can be achieved by inhibition of new vessel formation,¹ through anti-angiogenic agents, or by damaging existing blood vessel, through vascular disrupting agents (VDAs).²

In the field of anti-cancer drugs, several clinically useful drugs have been developed from natural source, by structural modification of natural compounds or by the synthesis of new compounds designed following a natural compound as model.

Abbreviations: ECs, endothelial cells; HUVECs, human umbilical vein ECs; MTD, maximum tolerated dose; SARs, structure–activity relationships; VTAs, vascular targeting agents; VDAs, vascular disrupting agents; 2-PPyQs, 2-phenyl-7*H*-pyrrolo[2,3-*h*]quinolinones; 7-PPyQs, 7-phenyl-3*H*-pyrrolo[3,2-*f*]quinolinones.

* Corresponding author. Address: Department of Pharmaceutical Sciences, Faculty of Pharmacy, University of Padova, via Marzolo 5, 35131 Padova, Italy. Tel.: +39 0498271603; fax: +39 0498275366.

E-mail address: mariagrazia.ferlin@unipd.it (M.G. Ferlin).

Microtubule-disrupting agents such as the natural compounds taxol, colchicines, vinca alkaloids, and flavonoids, induce extensive necrosis in tumors as a result of vascular collapse. Their main mechanism of action is believed to be impairment of tubulin assembly properties, leading to disruption of the microtubule network of proliferating endothelial cells (ECs). They have been reported to affect certain elements of angiogenic process, such as endothelial cell migration and in vitro capillary-like tube formation.³ Nevertheless, these effects are elicited at dosages close to the maximum tolerated dose (MTD). This limitation has been overcome by the development of second-generation tubulin depolymerizing agents, like DMXAA, CA4P, ZD6126, AVE8062A, and Oxi4503 (Fig. 1), which selectively disrupt the tumor vasculature at doses well below their MTD.⁴

Very recently, some progress in understanding the molecular and signaling mechanisms associated with endothelial activity of microtubule depolymerizing/destabilizing agents have been made.^{3,5}

Taking the natural flavone pharmacophore as a model, we have recently developed two series of pyrroloazaflavones (Fig. 2), namely 2-phenyl-1*H*-pyrrolo[2,3-*h*]quinolin-4(7*H*)ones and 7-phenyl-3*H*-pyrrolo[3,2-*f*]quinolin-9(6*H*)-ones (2-PPyQs and 7-PPyQs, respectively), as anti-cancer agents with an anti-microtubule mechanism,^{6–8} showing that the different geometry can account for the dissimilar effectiveness in antiproliferative activity on solid tumor cell lines: 7-PPyQs,⁸ especially 3-alkyl-substituted ones, are much more cytotoxic with nanomolar IC₅₀ than 2-PPyQs⁶, among which only some compounds were found to have low micromolar cytotoxicity.

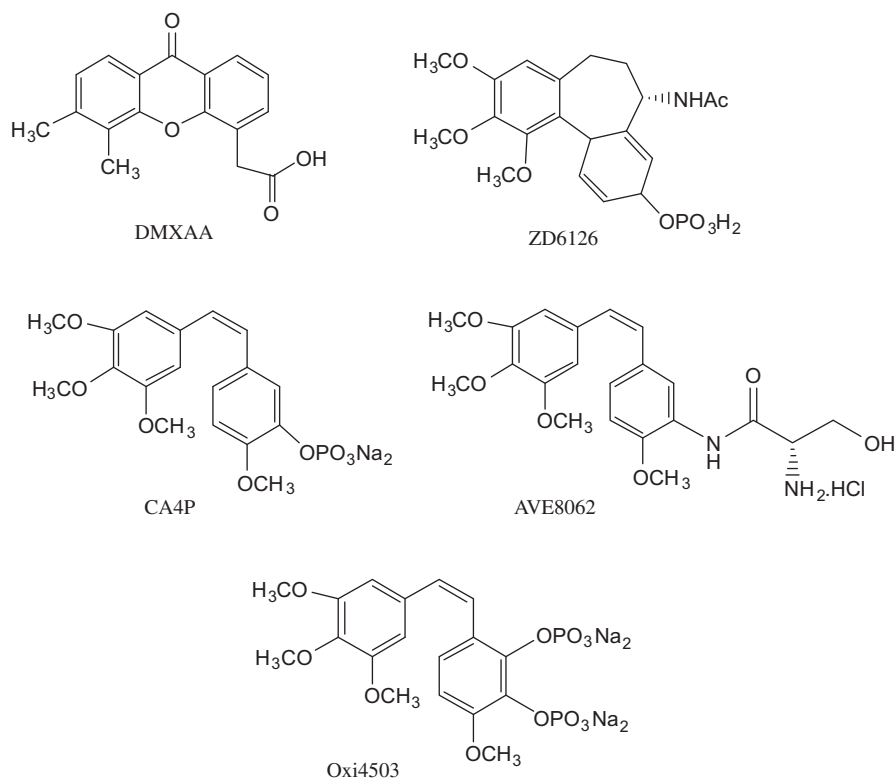


Figure 1. Structures of some anti-angiogenic agents mentioned in the text.

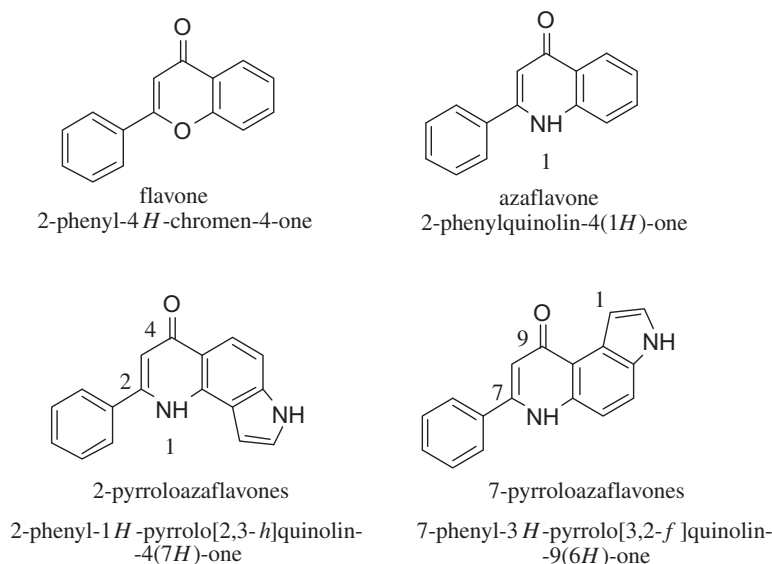


Figure 2. Structures of pyrroloazaflavones and their origin from the flavone pharmacophore.

However, the potential effect of pyrroloazaflavones on angiogenesis had not been studied. The aim of the current research was to evaluate the *in vitro* and *in vivo* effects on angiogenesis induced by some previously described 2-aryl-PyQs⁶ (**20–24**) belonging to the less cytotoxic series. Furthermore, some compounds with the same angular geometry **8**, **12**, **16**, and **19** were also prepared in order to have available a small library of differently substituted compounds (Table 1). Accordingly, the present study addressed growth inhibitory activity, migration and capillary-like tube formation *in vitro* on human umbilical vein ECs

(HUVECs) and the *in vivo* effects, evaluated by means of Matrigel plug assay.

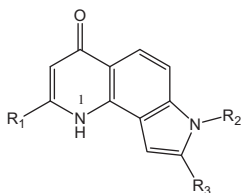
Vinblastine, known for its anti-angiogenic properties, was taken as reference compound.³

2. Materials and methods

Melting points were determined on a Gallenkamp MFB 595 010M/B capillary melting point apparatus, and are uncorrected. Infrared spectra were recorded on a Perkin-Elmer 1760 FTIR spec-

Table 1

Structure of the tested 2-aryl-pyrroloquinolinone derivatives **8**, **12**, **16**, and **19–24**^a



Compd	R ₁	R ₂	R ₃
8	2-Phenyl	Ethyl	
12	2-Phenyl	7-Methylcyclopropyl	
16	2-Phenyl	7-Ethylpropanoate	
19	2-Phenyl		CH ₃
20 ^a	2-Phenyl		
21 ^a	3'-OMe-2-phenyl		
22 ^a	3'-NO ₂ -2-phenyl		
23 ^a	2-Thiophen		
24 ^a	2-Pyrrolo		

^a Ref. 6.

trometer using potassium bromide pressed disks; all values are expressed in cm⁻¹. UV-vis spectra were recorded on a Perkin-Elmer Lambda UV/Vis spectrometer. ¹H NMR spectra were recorded on Varian Gemini (200 MHz) and Bruker (300 MHz) spectrometers, using the indicated solvents; chemical shifts are reported in δ (ppm) downfield from tetramethylsilane as internal reference. Coupling constants are given in Hertz. In the case of multiplets, chemical shift was measured starting from the approximate center. Integrals were satisfactorily in line with those expected on the basis of compound structure. Elemental analyzes were performed in the Microanalytical Laboratory, Department of Pharmaceutical Sciences, University of Padova, using a Perkin-Elmer elemental analyzer model 240B; results fell in the range of calculated values $\pm 0.4\%$. The analytical data are presented in detail for each final compound in the [Supplementary data](#). Mass spectra were obtained with a Mat 112 Varian Mat Bremen (70Ev) mass spectrometer and Applied Biosystems Mariner System 5220 LC/MS (nozzle potential 250.00). Column flash chromatography was performed on Merck silica gels (250–400 mesh ASTM); chemical reactions were monitored by analytical thin-layer chromatography (TLC) using Merck silica gel 60 F-254 glass plates with a 9:1 dichloromethane/methanol mixture as eluant, unless otherwise specified.

Solutions were concentrated in a rotary evaporator under reduced pressure. Starting materials were purchased from Aldrich Chimica, Acros, and solvents from Carlo Erba, Fluka, and Lab-Scan. DMSO was obtained anhydrous by distillation under vacuum and stored on molecular sieves.

2.1. N-(2-Methyl-3-nitro-phenyl)-acetimidic acid ethyl ester (**3**¹⁰)

In a tow-necked flask equipped with a Claisen condenser were placed commercial 2-methyl-3-nitroaniline (6.00 g, 39.4 mmol), *p*-toluenesulfonic acid (0.032 g, 0.2 mmol) and anhydrous triethyl-orthoformate (10 mL, $d = 0.885$, 54.7 mmol); the mixture was heated at 120 °C until all the ethanol had distilled off. Then, following vacuum distillation at 150 °C and 0.6 mmHg, the imidate ester (6.97 g) was collected. Yellow oily liquid; yield 92%; rf 0.80 (ethyl acetate/*n*-hexane 1:1); ¹H NMR (DMSO-*d*₆) δ 1.29 (t, 3H, $J = 7.05$ Hz, CH₃), 1.77 (s, 3H, CH₃), 2.15 (s, 3H, CH₃), 4.23 (q, 2H, $J = 7.05$ Hz, CH₂), 7.04 (dd, 1H, $J_{6,5} = 8.01$ Hz, $J_{6,4} = 0.96$ Hz, 6-H), 7.34 (dd, 1H, $J_{5,6} = 8.01$ Hz, $J_{5,4} = 8.01$ Hz, 5-H), 7.55 (dd, 1H, $J_{4,5} = 8.01$ Hz, $J_{4,6} = 0.96$, 4-H).

2.2. 2-Methyl-4-nitroindole (**4**¹⁰)

Without further purification, the imidate ester **3** was used in the reaction: in a 100 mL flask, 3.2 g (14.4 mmol) imidate ester in 12.0 mL anhydrous DMSO were treated with 3.0 mL diethyl oxalate (21.7 mmol, $d = 1.076$) in 8 mL anhydrous DMF and 1.58 g (18.8 mmol) potassium ethoxide at 0 °C. After 72 h at refluxing, the cooled red reaction mixture was poured onto ice/water and the nitro-indole separated as a red amorphous solid, which was collected and dried under vacuum at 30 °C. Subsequently it was purified by flash chromatography (ethyl acetate/*n*-hexane 1:1). Yield 25%; mp 192–94 °C; rf 0.63 (ethyl acetate/*n*-hexane 1:1); ¹H NMR (DMSO-*d*₆) δ 2.48 (s, 3H, CH₃), 6.79 (d, 1H, $J_{3,7} = 0.76$, 3-H), 7.18 (dd, 1H, $J_{6,7} = 8.01$ Hz, $J_{6,5} = 8.01$ Hz, 6-H), 7.74 (dd, 1H, $J_{7,6} = 8.01$ Hz, $J_{7,5} = 0.76$ Hz, 7-H), 7.98 (dd, 1H, $J_{5,6} = 8.01$ Hz, $J_{5,7} = 0.76$ Hz, 5-H), 11.98 (br s, 1H, NH).

2.3. General procedures for the synthesis of 1-substituted 4-nitroindole derivatives **5**, **9**, and **13**

In a round-bottomed flask, to 55.5 mmol of NaH (60% dispersion in mineral oil) a solution of 4-nitro-indole derivative, **2**⁶ (18.5 mmol) in 20–30 mL dry DMF was dropped and after 30 min at room temperature, a solution of halo-derivative in dry DMF was added and the reaction mixture was left stirred until the end (TLC). Then, the reaction mixture was workup in a standard way. The raw products were purified by flash chromatography.

2.3.1. 1-Ethyl-4-nitro-1H-indole (**5**)

Gummy brown solid; yield 78%; rf 0.62 (dichloromethane/ethyl acetate 8:2); ¹H NMR (DMSO-*d*₆) δ 1.38 (t, 3H, $J = 7.25$ Hz, CH₃), 4.33 (q, 2H, $J = 7.25$ Hz, CH₂), 7.05 (dd, 1H, $J_{3,2} = 3.25$ Hz, $J_{3,7} = 0.76$ Hz, 3-H), 7.35 (dd, 1H, $J_{6,5} = 8.01$ Hz, $J_{6,7} = 8.01$ Hz, 6-H), 7.81 (d, 1H, $J_{2,3} = 3.25$ Hz, 2-H), 8.05 (t, 2H, overlapping 5-H and 7-H); HRMS (ESI) calculated for C₁₀H₁₁N₂O₂ [M+H]⁺ m/z 191.078, found 191.081.

2.3.2. 1-Cyclopropylmethyl-4-nitro-1H-indole (**9**)

Orange liquid; yield 95%; rf 0.67 (toluene/*n*-hexane/ethyl acetate 1:1:0.3); ¹H NMR (DMSO-*d*₆) δ 0.42 (m, 2H, CH₂), 0.52 (m, 2H, CH₂), 1.26 (m, 1H, CH), 4.18 (d, 2H, $J = 7.05$, CH₂), 7.05 (dd, 1H, $J_{3,2} = 3.05$ Hz, $J_{3,7} = 0.76$ Hz, 3-H), 7.34 (dd, 1H, $J_{6,5} = 8.01$ Hz, $J_{6,7} = 8.01$ Hz, 6-H), 7.86 (d, 1H, $J_{2,3} = 3.05$ Hz), 8.26 (d, 1H, $J_{7,6} = 7.25$ Hz), 8.01 (d, 1H, $J_{5,6} = 8.01$ Hz, 5-H); HRMS (ESI) calculated for C₁₂H₁₃N₂O₂ [M+H]⁺ m/z 217.093, found 217.1007.

2.3.3. 3-(4-Nitro-indol-1-yl)-propionic acid ethyl ester (**13**)

Brown solid; yield 77%; mp 63–65 °C; rf 0.66 (benzene/*n*-hexane/ethyl acetate 1:1:1); ¹H NMR (DMSO-*d*₆) δ 1.08 (t, 3H, $J = 7.05$ Hz, CH₃), 2.88 (t, 2H, $J = 6.67$ Hz, CH₂), 3.99 (q, 2H, $J = 7.05$ Hz, CH₂), 4.56 (t, 2H, $J = 6.67$ Hz, CH₂), 7.03 (dd, 1H, $J_{3,2} = 3.05$ Hz, $J_{3,7} = 0.76$ Hz, 3-H), 7.35 (dd, 1H, $J_{6,5} = 8.01$ Hz, $J_{6,7} = 8.01$ Hz, 6-H), 7.78 (d, 1H, $J_{2,3} = 3.24$, 2-H), 8.08 (ddd, 2H, $J_{5,7} = 2.48$, $J_{7,5} = 2.48$ Hz, $J_{5,6} = 8.01$ Hz, $J_{7,6} = 8.01$ Hz, $J_{7,3} = 0.76$ Hz, 7-H and 5-H); HRMS (ESI) calculated for C₁₃H₁₅N₂O₄ [M+H]⁺ m/z 263.0987, found 263.1150.

2.4. General procedures for the synthesis of 4-amino-indole derivatives **6**, **10**, **14**, and **17**

A solution of a nitro-indole **5**, **9**, and **13** (5.87 mmol) in 400 mL ethanol was dropped into a suspension of 10% Pd/C (125 mg) saturated with H₂ in ethanol 200 mL. The mixture was stirred at room temperature with hydrogen at atmospheric pressure for 3 h, according to TLC analysis (ethyl acetate/*n*-hexane 1:3). After filtering off the catalyst, the filtrate was evaporated yielding the corresponding aminoindoles.

2.4.1. 1-Ethyl-1H-indol-4-ylamine (6)

Dense brown liquid; yield 91%; rf 0.42 (dichloromethane/ethyl acetate 8:2); ^1H NMR (DMSO- d_6) δ 1.30 (t, 3H, J = 7.25 Hz, CH_3), 4.07 (q, 2H, J = 7.25 Hz, CH_2), 5.33 (br s, 2H, NH_2), 6.16 (dd, 1H, $J_{7,6}$ = 7.43 Hz, $J_{7,3}$ = 0.76 Hz, 7-H), 6.44 (dd, 1H, $J_{3,2}$ = 3.24 Hz, $J_{3,7}$ = 0.76 Hz, 3-H), 6.64 (d, 1H, $J_{5,6}$ = 8.01 Hz, 5-H), 6.81 (dd, 1H, $J_{6,7}$ = 7.62 Hz, $J_{6,5}$ = 8.01 Hz, 6-H), 7.10 (d, 1H, $J_{2,3}$ = 3.24 Hz, 2-H); HRMS (ESI) calculated for $\text{C}_{10}\text{H}_{13}\text{N}_2$ $[\text{M}+\text{H}]^+$ m/z 161.103, found 161.1015.

2.4.2. 1-Cyclopropylmethyl-1H-indol-4-ylamine (10)

Dense brown liquid; yield 93%; rf 0.35 (toluene/*n*-hexane/ethyl acetate 1:1:0.3); ^1H NMR (DMSO- d_6) δ 0.33 (m, 2H, CH_2), 0.47 (m, 2H, CH_2), 1.19 (m, 1H, CH), 3.90 (d, 2H, CH_2 , J = 6.86 Hz), 5.15 (br s, 2H, NH_2), 6.15 (dd, 1H, $J_{7,6}$ = 7.44 Hz, $J_{7,3}$ = 0.76 Hz, 7-H), 6.49 (dd, 1H, $J_{3,2}$ = 3.14 Hz, $J_{3,7}$ = 0.76 Hz, 3-H), 6.65 (d, 1H, $J_{5,6}$ = 8.20 Hz, 5-H), 6.80 (dd, 1H, $J_{6,7}$ = 7.44 Hz, $J_{6,5}$ = 8.20 Hz, 6-H), 7.14 (d, 1H, $J_{2,3}$ = 3.14 Hz, 2-H); HRMS (ESI) calculated for $\text{C}_{12}\text{H}_{15}\text{N}_2$ $[\text{M}+\text{H}]^+$ m/z 187.119, found 187.1239.

2.4.3. 3-(4-Amino-indol-1-yl)-propionic acid ethyl ester (14)

Dense brown liquid; yield 98%; rf 0.25 (ethyl acetate/methanol 7:3); ^1H NMR (DMSO- d_6) δ 2.16 (s, 6H, $-(\text{CH}_3)_2$), 2.55 (t, 2H, J = 6.86 Hz, CH_2), 4.11 (t, 2H, J = 6.86 Hz, CH_2), 5.15 (br s, 2H, NH_2), 6.14 (dd, 1H, $J_{5,6}$ = 7.44 Hz, $J_{5,7}$ = 0.57 Hz, 5-H), 6.47 (dd, 1H, $J_{3,2}$ = 3.24 Hz, $J_{3,7}$ = 0.76 Hz, 3-H), 6.60 (d, 1H, $J_{7,6}$ = 8.20 Hz, 7-H), 6.80 (dd, 1H, $J_{6,5}$ = 7.63 Hz, $J_{6,7}$ = 8.01 Hz, 6-H), 7.09 (d, 1H, $J_{2,3}$ = 3.24 Hz, 2H); HRMS (ESI) calculated for $\text{C}_{13}\text{H}_{17}\text{N}_2\text{O}_2$ $[\text{M}+\text{H}]^+$ m/z 233.125, found 233.1245.

2.4.4. 2-Methyl-4-amino-1H-indole (17)

Dense orange liquid; yield 98%; rf 0.57 (ethyl acetate/*n*-hexane 8:2); ^1H NMR (DMSO- d_6) δ 2.30 (s, 3H, CH_3), 4.94 (br s, 2H, NH_2), 6.08 (dd, 1H, $J_{5,6}$ = 7.44 Hz, $J_{5,7}$ = 0.95 Hz, 5-H), 6.13 (d, 1H, $J_{3,7}$ = 0.95 Hz, 3-H), 6.30 (dd, 1H, $J_{7,6}$ = 8.01 Hz, $J_{7,5}$ = 0.76 Hz, 7-H), 6.65 (dd, 1H, $J_{6,5}$ = 8.01 Hz, $J_{6,7}$ = 8.40 Hz, 6-H), 10.57 (br s, 1H, NH); HRMS (ESI) calculated for $\text{C}_9\text{H}_{11}\text{N}_2$ $[\text{M}+\text{H}]^+$ m/z 147.088, found 147.0918.

2.5. General procedures for the synthesis of ethyl acrylate derivatives 7, 11, 15, and 18

In a round-bottomed flask, 3–4 mmol of 3-substituted-amino-indole **6**, **10**, **14**, and **17** in 10–20 mL absolute ethanol were condensed with an equimolar quantity of commercial ethyl benzoylacetate and with 1 mL glacial acetic acid and 100 mg drierite. The mixture was refluxed for about 24 h (TLC), and after removing the drierite; the resulting solution was evaporated to dryness and the residue used in the following reaction without any purification. A sample was purified for analysis by flash chromatography.

2.5.1. 3-(1-Ethyl-1H-indole-4-ylamino)-3-phenyl-acrylic acid ethyl ester (7)

Yield was not estimated. Dark red vitreous solid; rf 0.96 (dichloromethane/ethyl acetate 8:2); ^1H NMR (DMSO- d_6) δ 1.25 (t, 3H, J = 7.05 Hz, CH_3), 1.36 (t, 3H, J = 7.25 Hz, CH_3), 3.17 (q, 2H, J = 7.25 Hz, CH_2), 3.99 (d, 2H, J = 7.05 Hz, CH_2), 4.97 (s, 1H, $-\text{C}=\text{CH}-$), 5.93 (d, 1H, $J_{5,6}$ = 7.63 Hz, 5-H), 6.53 (dd, 1H, $J_{3,2}$ = 3.05 Hz, $J_{3,7}$ = 0.76 Hz, 3-H), 6.75 (dd, 1H, $J_{6,5}$ = 7.78 Hz, $J_{6,7}$ = 8.20 Hz, 6-H), 7.40 (d, 1H, $J_{2,3}$ = 3.05 Hz, 2-H), 7.52 (m, 6H, ar); HRMS (ESI) calculated for $\text{C}_{21}\text{H}_{23}\text{N}_2\text{O}_2$ $[\text{M}+\text{H}]^+$ m/z 335.171, found 335.1712.

2.5.2. 3-(1-Cyclopropylmethyl-1H-indole-4-ylamino)-3-phenyl-acrylic acid ethyl ester (11)

Yield was not estimated. Yellow oily liquid; rf 0.78 (toluene/*n*-hexane/ethyl acetate 1:1:0.3); ^1H NMR (DMSO- d_6) δ 0.36

(m, 2H, CH_2), 0.49 (m, 2H, CH_2), 1.24 (m, t, 4H, overlapping, J = 7.05 Hz, CH and CH_3), 3.99 (d, 2H, J = 6.86 Hz, $\text{N}-\text{CH}_2$), 4.16 (q, 2H, J = 7.05 Hz, CH_2), 4.97 (s, 1H, $-\text{CH}-$), 5.93 (d, 1H, $J_{7,6}$ = 7.72 Hz, 7-H), 6.54 (dd, 1H, $J_{3,2}$ = 3.14 Hz, $J_{3,7}$ = 0.76 Hz, 3-H), 6.75 (dd, 1H, $J_{6,7}$ = 7.72 Hz, $J_{6,5}$ = 8.20 Hz, 6-H), 7.13 (d, 1H, $J_{5,6}$ = 8.20 Hz, 5-H), 7.33 (m, 5H, overlapping), 7.45 (d, 1H, $J_{2,3}$ = 3.14 Hz, 2-H), 10.47 (br s, 1H, NH); HRMS (ESI) calculated for $\text{C}_{23}\text{H}_{24}\text{N}_2\text{O}_2$ $[\text{M}+\text{H}]^+$ m/z 361.187, found 361.1928.

2.5.3. 3-[1-(2-Ethoxycarbonyl-ethyl)-1H-indole-4-ylamino]-3-phenyl-acrylic acid ethyl ester (15)

Yield was not estimated. Dense brown liquid; rf 0.51 (ethyl acetate/methanol 7:3); ^1H NMR (DMSO- d_6) δ 1.11 (t, 3H, J = 7.05 Hz, CH_3), 1.16 (t, 3H, J = 7.05 Hz, CH_3), 2.80 (t, 2H, J = 6.67 Hz, CH_2), 4.01 (q, 2H, J = 7.05 Hz, CH_2), 4.13 (q, 2H, J = 7.05 Hz, CH_2), 4.38 (t, 2H, J = 6.67 Hz, CH_2), 4.98 (s, 1H, NH), 5.94 (d, 1H, $J_{7,6}$ = 7.44 Hz, 7-H), 6.54 (d, 1H, $J_{3,2}$ = 3.24 Hz, 3-H), 6.75 (dd, 1H, $J_{6,7}$ = 7.82 Hz, $J_{6,5}$ = 8.20 Hz, 6-H), 7.10 (d, 1H, $J_{5,6}$ = 8.20 Hz, 5-H), 7.33 (m, 6H, overlapping), 10.45 (br s, 1H, NH); HRMS (ESI) calculated for $\text{C}_{24}\text{H}_{27}\text{N}_2\text{O}_4$ $[\text{M}+\text{H}]^+$ m/z 407.1926, found 407.1997.

2.5.4. 3-(2-Methyl-1H-indole-4-ylamino)-3-phenyl-acrylic acid ethyl ester (18)

Yield was not estimated. Brown dense liquid; rf 0.76 (ethyl acetate/*n*-hexane 1:1); ^1H NMR (DMSO- d_6) δ 1.24 (t, 3H, J = 7.05 Hz, CH_3), 2.39 (s, 3H, CH_3), 4.03 (q, 2H, J = 7.25 Hz, CH_2), 4.92 (s, 1H, $-\text{CH}$), 5.97 (d, 1H, $J_{5,6}$ = 7.78 Hz, 5-H), 6.22 (s, 1H, 3-H), 6.60 (dd, 1H, $J_{6,7}$ = 7.78 Hz, $J_{6,5}$ = 7.78 Hz, 6-H), 6.89 (d, 1H, $J_{7,6}$ = 7.78 Hz, 7-H), 7.33 (m, 5H, ar), 10.41 (br s, NH), 11.43 (br s, NH); HRMS (ESI) calculated for $\text{C}_{20}\text{H}_{21}\text{N}_2\text{O}_2$ $[\text{M}+\text{H}]^+$ m/z 321.156, found 321.1573.

2.6. General procedures for the synthesis of 2-phenyl-pyrroloquinolinones 8, 12, 16, and 19

In a two-necked round-bottomed flask, 50 mL of diphenyl ether were heated to boiling temperature; 1–2 mmol of acrylates **7**, **11**, **15**, and **18** were then added portion-wise and the mixture was refluxed for 30 min. After cooling to 60 °C, the separated precipitate was collected by filtration and washed many times with diethyl ether. In all cases, the collected products were purified by flash chromatography (ethyl acetate/methanol 9:1). Yields were estimated from corresponding amino compound intermediates.

2.6.1. 7-Ethyl-2-phenyl-1H,7H-pyrrolo[2,3-*h*]quinolin-4-one (8)

Yield 37%; rf 0.51 (ethyl acetate/methanol 9:1), mp 250–261 °C; IR (KBr) 1628 cm^{-1} (CO); IR (KBr) 1628 cm^{-1} ; ^1H NMR (DMSO- d_6) δ 1.34 (t, 3H, J = 7.25 Hz, CH_3), 4.22 (q, 2H, J = 7.25 Hz, CH_2), 6.21 (d, 1H, $J_{3,1}$ = 1.14 Hz, 3-H), 7.07 (d, 1H, $J_{5,6}$ = 8.96 Hz, 5-H), 7.29 (m, 2H, 6-H and 9-H overlapping), 7.42 (d, 1H, $J_{8,9}$ = 3.24 Hz, 8-H), 7.51 (m, 5H, aryl), 12.03 (s, 1H, NH quinolinic); ^{13}C NMR (DMSO- d_6) δ 16.07 (CH_3), 42.30 (CH_2), 100.72 (C-9a), 107.77 (C-9), 17.77 (C-4a), 113.33 (C-6), 116.90 (C-6', C-2'), 117.34 (C-8), 121.15 (C-3', C-5'), 128.54 (C-4'), 129.68 (C-9b e C-1'), 129.82 (C-6a), 129.96 (C-5), 134.83 (C-2), 138.08 (C-4), 139.67 (C-8), 157.12 (C-3', C-5'), 165.23 (C-4'); HRMS (ESI) calculated for $\text{C}_{19}\text{H}_{16}\text{N}_2\text{O}$ $[\text{M}+\text{H}]^+$ m/z 289.1335, found 289.1334.

2.6.2. 7-Cyclopropylmethyl-2-phenyl-1H,7H-pyrrolo[2,3-*h*]quinolin-4-one (12)

Yield 35%; rf 0.50 (ethyl acetate/methanol 9:1); mp 260–262 °C; IR (KBr) 1627 cm^{-1} (CO); ^1H NMR (DMSO- d_6) δ 0.41 (m, 2H, CH_2), 0.52 (m, 2H, CH_2), 1.26 (m, 1H, CH), 4.14 (d, 2H, CH_2), 6.23 (s, 1H, 4-H), 7.38 (d, 1H, $J_{9,8}$ = 3.24 Hz, 9-H), 7.51 (d, 1H, $J_{8,9}$ = 3.24 Hz, 8-H), 7.54 (d, 1H, $J_{6,5}$ = 8.86 Hz, 6-H), 7.60 (m, 3H, aryl), 7.78 (m, 2H, aryl), 7.87 (d, 2H, $J_{5,6}$ = 8.96 Hz, 5-H), 11.52 (br

s, NH quinolinic); ^{13}C NMR (CDCl_3): δ 4.01 (2(CH_2), 11.35 ($-\text{CH}-$), 51.03 (CH_2), 99.21, 107.93, 109.04, 116.36, 118.48, 119.11, 126.97, 129.06, 130.08, 134.85, 135.11, 137.48, 148.53, 178.81; HRMS (ESI) calculated for $\text{C}_{21}\text{H}_{18}\text{N}_2\text{O}$ $[\text{M}+\text{H}]^+$ m/z 315.1453, found 315.1492.

2.6.3. 3-(4-Oxo-2-phenyl-1,4-dihydro-pyrrolo[2,3-*h*]quinolin-7-propionic acid ethyl ester (16)

Yield 30%; rf 0.50 (ethyl acetate/methanol 9:1); mp 260–262 °C; IR (KBr) 1627 cm^{-1} (CO); ^1H NMR ($\text{DMSO}-d_6$) δ 0.41 (m, 2H, CH_2), 0.52 (m, 2H, CH_2), 1.26 (m, 1H, CH), 4.14 (d, 2H, CH_2), 6.23 (s, 1H, 4-H), 7.38 (d, 1H, $J_{9,8} = 3.24\text{ Hz}$, 9-H), 7.51 (d, 1H, $J_{8,9} = 3.24\text{ Hz}$, 8-H), 7.54 (d, 1H, $J_{6,5} = 8.86\text{ Hz}$, 6-H), 7.60 (m, 3H, aryl), 7.78 (m, 2H, aryl), 7.87 (d, 2H, $J_{5,6} = 8.96\text{ Hz}$, 5-H), 11.52 (br s, NH quinolinic); ^{13}C NMR (CDCl_3): δ 4.01 (2(CH_2), 11.35 ($-\text{CH}-$), 51.03 (CH_2), 99.21, 107.93, 109.04, 116.36, 118.48, 119.11, 126.97, 129.06, 130.08, 134.85, 135.11, 137.48, 148.53, 178.81; HRMS (ESI) calculated for $\text{C}_{21}\text{H}_{18}\text{N}_2\text{O}$ $[\text{M}+\text{H}]^+$ m/z 315.1453, found 315.1492.

2.6.4. 8-Methyl-2-phenyl-1*H*,7*H*-pyrrolo[2,3-*h*]quinolin-4-one (19)

Yield 30%; rf 0.55 (ethyl acetate/methanol 9:1); mp 233–235 °C; IR (KBr) 1628 cm^{-1} (CO); ^1H NMR ($\text{DMSO}-d_6$) δ 2.43 (s, 3H, CH_3), 6.20 (s, 1H, 3-H), 7.05 (s, 1H, 9-H), 7.27 (d, 1H, $J_{6,5} = 8.58\text{ Hz}$, 6-H), 7.57 (m, 3H, aryl), 7.76 (m, 3H, aryl), 11.38 (br s, 1H, NH pyrrolic), 11.46 (br s, 1H, NH, quinolinic); ^{13}C NMR (CDCl_3) δ 13.54, 73.54, 99.93, 108.67, 111.54, 117.59, 118.26, 129.09, 130.05, 131.49, 136.04, 136.31, 136.79, 139.46, 152.36, 180.37, 205.57; HRMS (ESI) $[\text{M}+\text{H}]^+$ calculated for $\text{C}_{18}\text{H}_{14}\text{N}_2\text{O}$ m/z 275.1140, found 275.1179.

Elemental analysis data for new compounds are given in Supplementary data.

3. Biology

3.1. Cell cultures

Primary cultures of human umbilical vein ECs (HUVECs) were obtained by enzymatic digestion of umbilical vein endothelial layer with 0.1% collagenase IV solution (Sigma Aldrich) and the cells were seeded on Petri dishes previously coated with fibronectin (1 $\mu\text{g/mL}$) and cultured with Endothelial Cell Growth Medium MV₂ (basal medium, Promocell) supplemented with 5% FCS, ascorbic acid (1 $\mu\text{g/mL}$), hFGF-2 (10 ng/mL), hEGF (5 ng/mL), hydrocortisone (0.2 $\mu\text{g/mL}$), R³-IGF-1 (20 ng/mL), VEGF (0.5 ng/mL) (endothelial MV₂ medium kit) (Promocell), and 1% antibiotic solution containing streptomycin sulfate (10 ng/mL), amphotericin-B (250 ng/mL), and penicillin (100 U/mL) (Sigma). Cultures were incubated at 37 °C in a humidified atmosphere. HUVECs were used from 2nd to 4th passage and harvested at 80% confluence.

3.2. Growth inhibitory activity assay

The 3-(4,5-dimethylthiazol-2-yl)-2,5-dimethyltetrazolium bromide (MTT)-tetrazolium dye assay was used to evaluate the growth inhibitory activity of the compounds at various concentrations. HUVECs ($2 \times 10^4\text{ cell/cm}^2$) were seeded into 96-well plates. After a 24 h incubation period, media were replaced with ones containing or not various concentrations (from 10 to $10^{-5}\text{ }\mu\text{M}$) of the tested compounds. Alternatively, 50 ng/mL FGF-2 (Sigma) alone or with the compounds at the highest concentration not inducing decrease in cell viability ($10^{-5}\text{ }\mu\text{M}$ vinblastine; $10^{-4}\text{ }\mu\text{M}$ 2-PPyQ **20**; $10^{-3}\text{ }\mu\text{M}$ 3'-NO₂- **22**; $10^{-2}\text{ }\mu\text{M}$ 3'-MeO- **21**, 7-*c*-Propylmet- **12**, 7-EtPropanoate- **16**, and 7-Et- **8** 2-PPyQs) were simultaneously added to the media. After 20 h incubation, cells were treated with MTT (0.5 mg/

mL, Sigma) for 4 h. Formazane precipitates were dissolved in 2-propanol acid (0.04 M HCl in 2-propanol; Sigma) and optical density was measured at 570 nm using a Microplate auto reader EL 13 (BIO-TEK instruments Inc. Winooski, Vermont, USA). Results were expressed as percent change from control non-treated cultures as well as IC₅₀, that is, the concentrations of the agents (μM), which induced a 50% reduction of viability in comparison with non-treated cultures. Both IC₅₀ values and non-cytotoxic concentrations were obtained from dose-response curves. The linearity of absorbance of formazan over a range of 5×10^3 to 50×10^4 cells was established by determining the linear coefficient (0.9858).

3.3. Pro-apoptotic assay

HUVECs ($2 \times 10^4\text{ cell/cm}^2$) were seeded onto fibronectin coated 8-well chamber slides (BD) and incubated overnight at 37 °C. Then, cells were washed and treated for 24 h with IC₅₀ concentration of the tested compounds dissolved in basal medium. Cultures were fixed in 3% paraformaldehyde for 1 h at room temperature and apoptosis was detected by TUNEL assay, using the Roche In situ Cell Death detection kit. Briefly, cells were permeabilized with 0.1% Triton X-100 (Sigma) in 0.1% sodium citrate solution for 2 min on ice, washed twice with PBS and then incubated with a mixture of terminal deoxynucleotidyl transferase and fluorescein-labeled nucleotides for 1 h at 37 °C. The total number of nuclei were visualized by fluoresce microscopy after incubation of cultures with DAPI for 10 min at room temperature. The apoptotic rate (percent of TUNEL-positive cells) was estimated by counting 10 fields for each sample and three wells were employed for each experimental condition. Results were expressed as percent change from control cultures grown with basal medium. In the control non-treated cultures, negligible apoptotic rate was seen.

3.4. Migration assay

Cell migration was evaluated using a modified Boyden chamber. HUVECs ($1.5 \times 10^4\text{ cell/cm}^2$) were seeded on the upper side of 5.0 μm pore Transwell insert (Corning Inc.) in basal medium supplemented with 1% FCS with or without not cytotoxic concentration of the tested compounds. Inserts were placed in a 24-well plate containing medium supplemented with 1% FCS and growth factors (lower chamber). After 4 h. cultures were fixed in 10% formaldehyde (Sigma) and the upper membrane of the insert was swabbed to removed non-migrated cells. The membrane was cut from the insert and mounted with DAPI. HUVECs migration was quantified by counting the number of nuclei in the lower side of the membrane in five random fields per insert (100 \times magnification) by fluoresce microscopy. Experiments were repeated five times. Results were expressed as percent change from control not treated cultures.

3.5. Morphogenesis analysis

Morphogenesis analysis was carried out seeding HUVECs on Matrigel (BD Biosciences). Matrigel was thawed on ice overnight, spread evenly over each well (50 μL) of a 24-well plate, and allowed to polymerized for 30 min at 37 °C. HUVECs ($2.5 \times 10^4\text{ cells/cm}^2$) were seeded on Matrigel and cultured in basal medium supplemented with 1% FCS and with or without not cytotoxic concentrations of the tested compounds, as above detailed, FGF-2 (50 ng/mL), and FGF-2 plus compounds. After 18 h of incubation at 37 °C, cultures were fixed in 2% glutaraldehyde in cacodylate buffer, pH 7.2 and then photographed (five fields for each well: the four quadrants and the center) at a magnification of 50 \times . Phase contrast images were recorded using a digital camera and save as TIFF files. Image analysis was carried out using the ImageJ image analysis software and the following dimensional parameters (percent area cov-

ered by HUVECs and total length of HUVECs network per field), and topological parameters (number of meshes and branching points per fields) were estimated. Values were expressed as percent change from control cultures grown with basal medium or FGF-2.

3.6. In vivo Matrigel plug assay

Three-month-old C57/BL6 mice were anesthetized with isoflurane (2–3%) via nose cone and 100% oxygen used as the carrier gas; the back was shaved and disinfected with ethyl alcohol. A total of 0.5 mL of Matrigel, mixed with 12 U.I. heparin (Vister) with or without 200 ng/plug FGF-2 and 0.01 μ M tested compounds, was injected subcutaneously on dorsal area. After injection, the Matrigel polymerized forming a plug. After 7 days, the animals were sacrificed and the plugs were carefully removed and steeped in 300 μ L/plug Brij-35 0.1% solution in PBS at 4 °C overnight. Hemoglobin concentration was analyzed using Drabkin's Reagent kit (Sigma). The optical density was read at 540 nm using a Microplate auto reader EL 13. The results were expressed as mg/mL hemoglobin.

4. Statistical analysis

All results were expressed as mean \pm SD of three separate experiments. Their statistical comparison was performed by analysis of variance followed by Student's *t*-test.

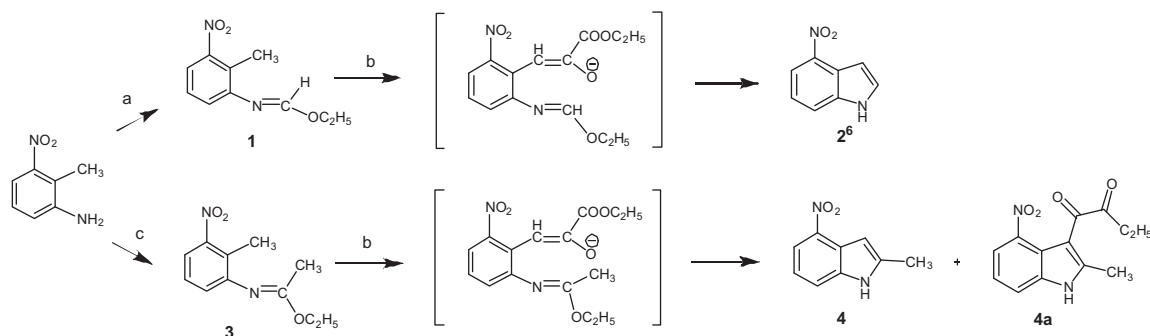
5. Results

5.1. Chemistry

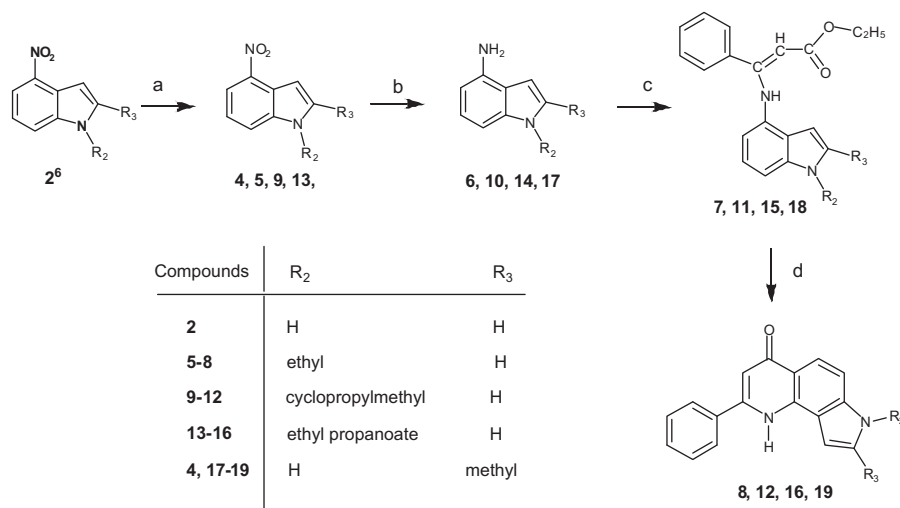
The new 2-PPyQs, substituted at 7*N*-pyrrole (**8**, **12**, and **16**) and at position 8 (**19**), were synthesized according to the routes shown in Scheme 1: in section A, 4-nitroindoles **2** and **4** were obtained by the Sand and Bergman procedure.^{9,10} Commercial 3-nitro-2-methyl-aniline was transformed into imidate esters **1** (85%) and **3** (92%) by treatment with triethyl orthoformate or orthoacetate, respectively, in the presence of *p*-toluensulfonic acid. The imidates furnished cyclization products **2**⁶ (64%) and **4** (25%) when reacted with potassium *tert*-butoxide and diethyloxalate in anhydrous DMF and DMSO. It is interesting to note that in the case of formimidate **1**, the only one cyclized 4-nitro-indole **2** was isolated from the reaction mixture, whereas in the case of methyl imidate **3**, a mixture was obtained of **4** and the 3-diketoethyl ester derivative **4a**, which was isolated and characterized (Supplementary data). This finding confirms the reaction mechanism proposed by Sand and Bergman.^{9,10}

In section B, nitroindole **2** was alkylated to 1*N*-alkyl derivatives **5**, **9**, and **13** by appropriate halogenated compounds and NaH in DMF or, in the case of **13**, toluene, in order to prevent hydrolysis of propanoate ethyl ester to the corresponding propanoic acid derivative. Next, catalytic reductions of **5**, **9**, **13**, and **4** were all per-

A] Synthetic route to 4-nitroindoles **2**⁶ and **4**



B] Synthesis of substituted 2-phenyl-pyrroloquinolinones **8**, **12**, **16** and **19**



Scheme 1. (A) Synthetic route to 4-nitroindoles **2**⁶ and **4**. Reagents and conditions: (a) triethyl ortho-formate, *p*-toluensulfonic acid monohydrate, 120 °C; (b) potassium *tert*-butoxide, diethyl oxalate, anhydrous DMF/DMSO mixture, 50 °C; (c) triethyl *ortho*-acetate, *p*-toluensulfonic acid monohydrate, 120 °C. (B) Synthesis of substituted 2-phenyl-pyrroloquinolinones **8**, **12**, **16**, and **19**. Reagents and conditions: (a) bromoethane or (bromomethyl)cyclopropane, NaH/DMF or ethyl acrylate NaH/toluene, reflux; (b) H₂ atm, Pd/C 10%, ethanol, 40 °C; (c) ethyl benzoylacetate, absolute ethanol, acetic acid, drierite, reflux; (d) diphenyl ether, 250 °C.

formed with H₂ and Pd/C 10%, leading to almost pure 4-amino-indoles **6**, **10**, **14**, and **17** in high yields. The two final steps, condensation with ethyl benzoylacetate and thermal intramolecular cyclization, were performed following previously published protocols,^{6–8} furnishing first enamine derivatives **7**, **11**, **15**, and **18** and then 2-PPyQs **8**, **12**, **16**, and **19**.

Table 2

In vitro inhibitory effects on cell growth of HUVECs by compounds **8**, **12**, **16**, **19–24**

Compd	IC ₅₀ ^a (μM)
7-Et-2-PPyQ 8	8.1 ± 1.1
7-MeCypr-2-PPyQ 12	4.2 ± 0.7
7-EtPr-2-PPyQ 16	5.7 ± 0.8
8-Me-2-PPyQ 19	>10 ^b
2-PPyQ 20	4.3 × 10 ⁻² ± 1.1 × 10 ⁻²
3'-MeO-2-PPyQ 21	5.8 ± 0.9
3'-NO ₂ -2-PPyQ 22	0.45 ± 0.19
2-Th-2-PPyQ 23	>10 ^b
2-Py-2-PPyQ 24	>10 ^b
Vinblastine	4.9 × 10 ⁻² ± 0.9 × 10 ⁻²

^a Values are means ± SD of at least three independent experiments.

^b IC₅₀ not determined, because <50% inhibition was observed at highest tested concentration (10 μM). Higher concentrations were not used, to avoid precipitation of compounds in culture medium.

5.2. Biology

5.2.1. Growth inhibitory effects of 2-PPyQs on endothelial cells

Inhibitory effects on cell growth were determined by MTT assay (Table 2). Results showed that derivatives, bearing a phenyl group at the 2-position, were more cytotoxic than those with a thiophene and pyrrolo ring **23** and **24**, respectively. Compound **20** had an IC₅₀ value of 4.3 × 10⁻² μM similar to that determined for vinblastine, 4.9 × 10⁻² μM (Table 2). The presence of substituents at the phenyl group, compounds **21** and **22**, decreased viability (IC₅₀ 5.2 and 0.45 μM, respectively), and, consequently, the corresponding IC₅₀ values were from 10- to 100-fold lower than that calculated for compound **20**. Derivative **19**, bearing the methyl group at the 8-position, was almost ineffective (IC₅₀ >10 μM). In view of the inhibitory effect on HUVEC cell growth, the more active compounds, **8**, **12**, **16**, **20–22**, were selected for further studies.

5.2.2. Effects on in vitro angiogenesis

It was evaluated whether the 2-PPyQ derivatives **8**, **12**, **16**, **19–24** could counteract the angiogenic effects of FGF-2, which represents one of the most important growth factors involved in the angiogenic process. The increase in cell proliferation induced by FGF-2 was completely reversed by all assayed compounds at non-cytotoxic concentrations (see growth inhibition assay). Compounds **8** and **20** appeared more, while compounds **12**, **16**, and **22** less effective than vinblastine (Fig. 3).

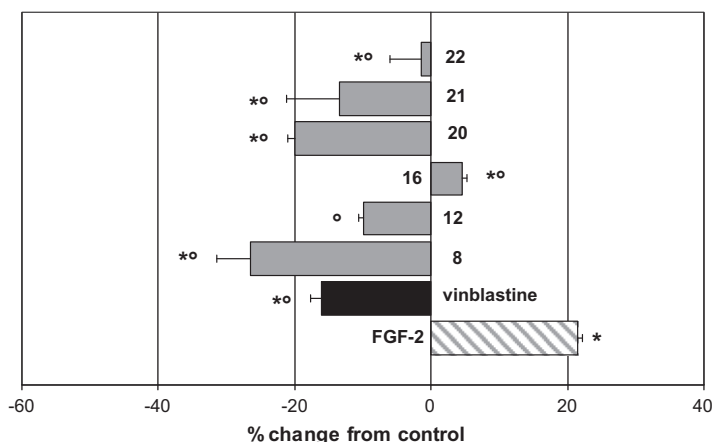


Figure 3. Effects of compounds **8**, **12**, **16**, and **20–22** on HUVEC proliferation incubated for 24 h with 50 ng/mL FGF-2. Data are means ± SD of three separate experiments. **p* < 0.05 versus control; **p* < 0.05 versus FGF-2, Student's *t*-test.

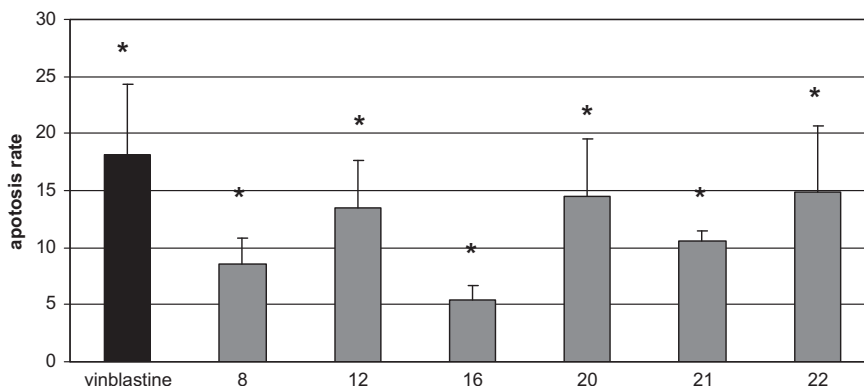


Figure 4. Pro-apoptotic effects of compounds **8**, **12**, **16**, and **20–22** on HUVECs. Cells were treated for 24 h with compounds at IC₅₀ concentrations. After the incubation period, cultures were fixed and apoptosis was detected by TUNEL assay. Results, expressed as percent change from untreated control cultures (taken as 0), are means ± SD of at least three independent experiments. **p* < 0.05 versus control cultures, Student's *t*-test.

5.2.3. Pro-apoptotic effects of 2-PPyQs

To determine the mode by which these 2-PPyQs decreased cell growth, their effect on apoptosis was assessed by TUNEL assay. The cytotoxic effects of 2-PPyQ **8**, **12**, **16**, and **20–22**, such as vinblastine, seemed to be related to their pro-apoptotic activity. All compounds induced increases in the apoptotic rate when compared with untreated cultures (Fig. 4).

5.2.4. Effects on endothelial cell migration

Cell migration represents an important step in the angiogenic process. All tested compounds **8**, **12**, **16**, and **20–22** induced signif-

icant inhibitory effects on HUVEC migration at the highest concentration not inducing decrease in cell growth (see growth inhibition assay) compared with that determined in control cultures (Fig. 5). Nevertheless, only compound **8** was as effective as vinblastine, the other derivatives appeared to be less effective.

5.2.5. Effects of 2-PPyQs on capillary-like formation

The final event of angiogenesis is the organization of ECs in a three-dimensional network of capillary-like structures. In vitro HUVECs seeded on a thick layer of Matrigel, rapidly align and within a few hours form a highly branched network of capillaries, which is complete in 24 h. Therefore, we examined whether 2-PPyQs at non-cytotoxic concentrations (see growth inhibition assay) were able to affect the formation of these structures. Morphogenesis on Matrigel was inhibited by vinblastine, which significantly decreased both dimensional (percent area covered by HUVECs and total length of network per field, A and B in Fig. 6, respectively) and topological parameters (number of meshes and branching points per field, C and D in Fig. 6, respectively) of the capillary-like network. Compounds **8**, **12**, **16**, and **20** were more effective than vinblastine, leading to a drastic reduction in the number of capillary-like structures, while **21** and **22** only affected topological parameters.

To further investigate whether 2-PPyQs exhibit anti-angiogenic activity, their in vitro effects on capillary-like formation after treatment with the pro-angiogenic FGF-2, were also evaluated. The FGF-2-induced increases in both dimensional and topological parameters were completely abolished by vinblastine, and by compounds **16** and **22** (A, B and C, D in Fig. 7, respectively). The compound **20** affected all parameters except for the numbers of branching points per field (D in Fig. 7). The compound **21** had no effect, whereas the compounds **8** and **12** decreased only the number of branching points.

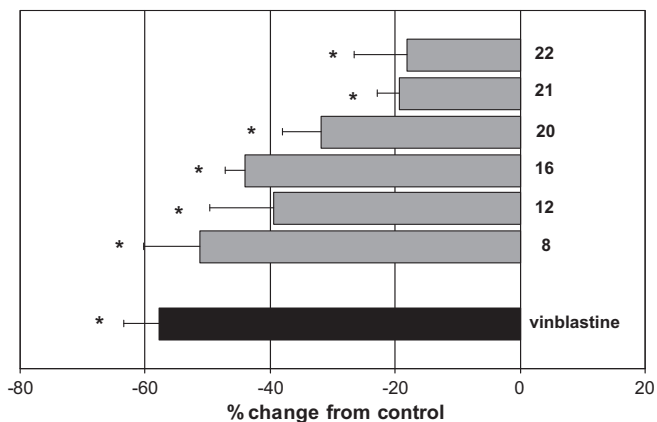


Figure 5. HUVEC migration through a 5.0 μm pore after 4 h from seeding. Cells were treated with compounds **8**, **12**, **16**, and **20–22** at highest concentration not inducing decrease in cell viability. Results, expressed as percent change from untreated control cultures (taken as 0), are means \pm SD of at least three independent experiments. $p < 0.05$ versus control cultures, Student's t -test.

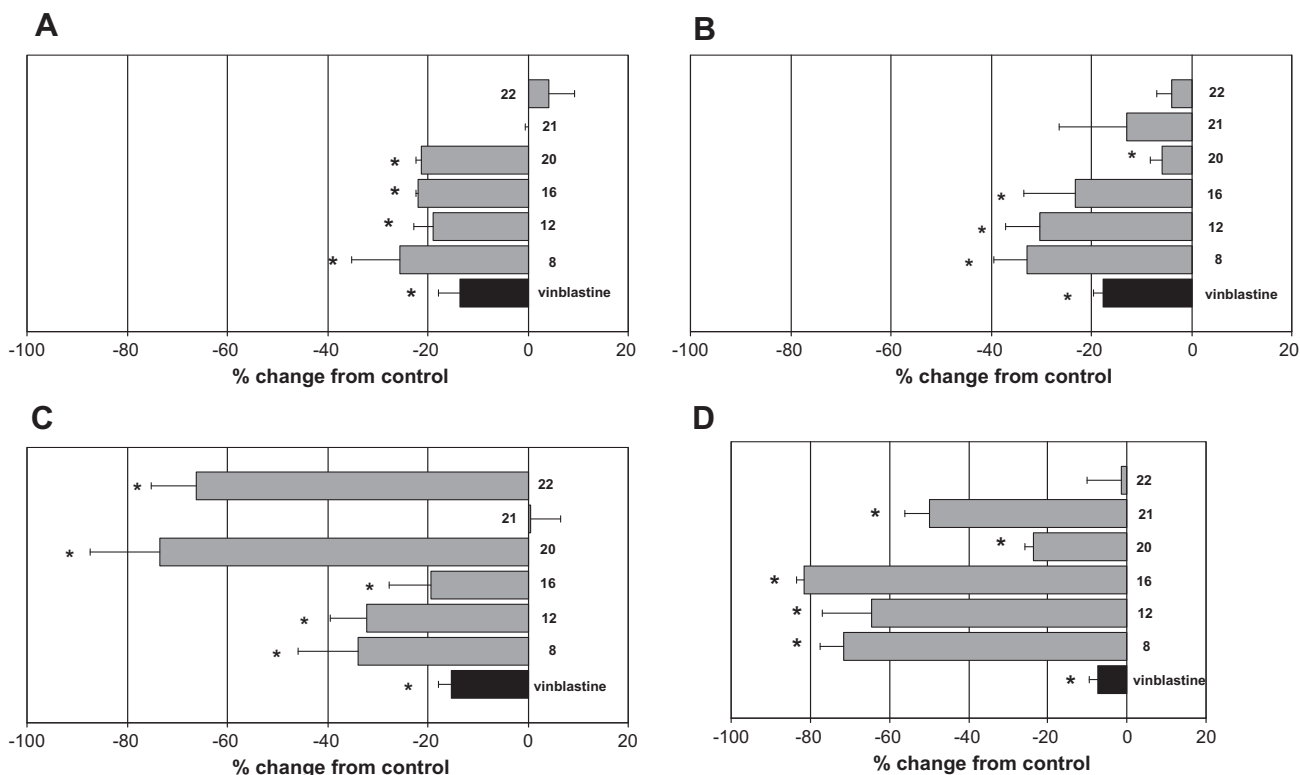


Figure 6. Quantitative analysis of effects of compounds **8**, **12**, **16**, and **20–22** on dimensional (A: percent area covered by HUVECs; B: total length per field) and topological parameters (C: numbers of meshes per field; D: numbers of branching points per field) of HUVEC meshwork. Cultures were treated with compounds at highest concentration not inducing decrease in cell viability. Bars are means \pm SD of three separate experiments. $*p < 0.05$ versus control cultures, Student's t -test.

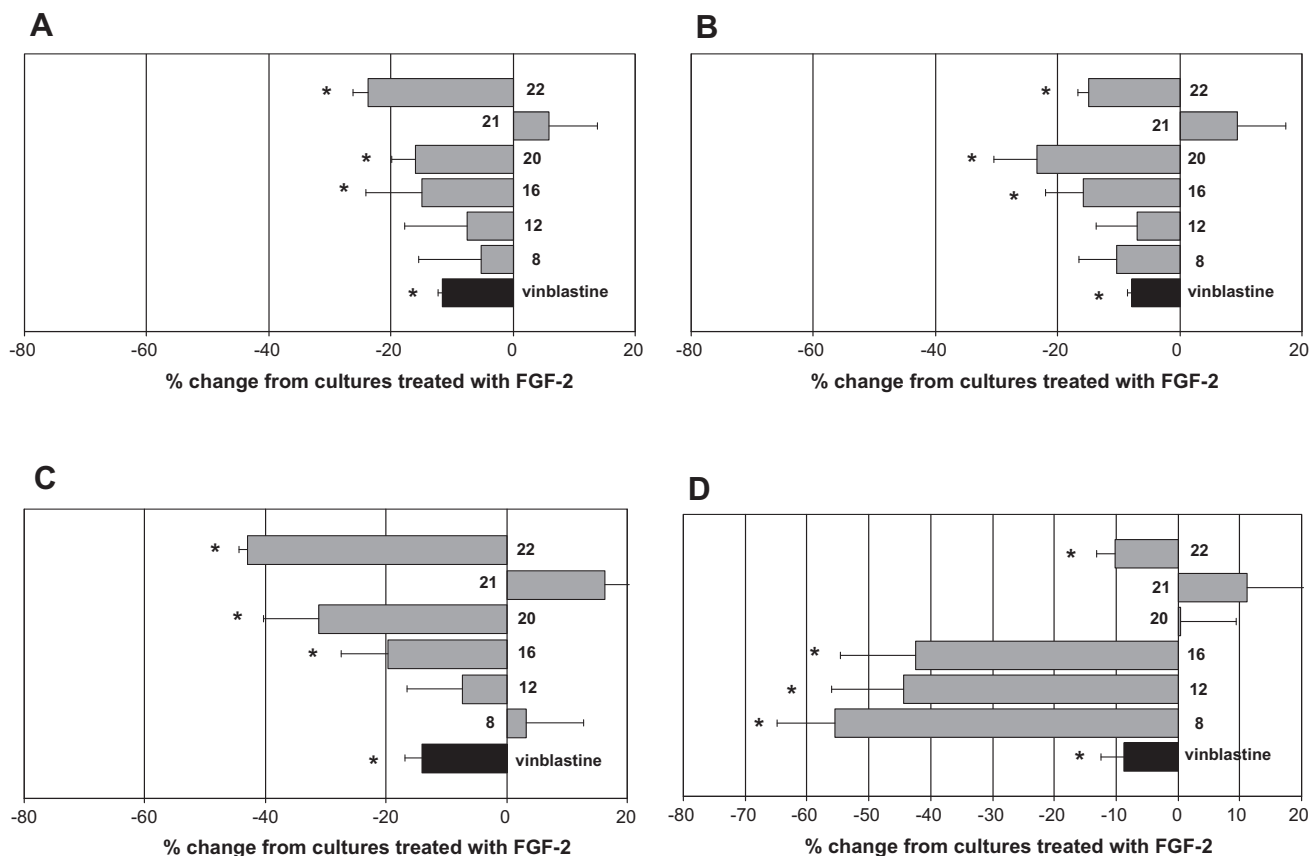


Figure 7. Quantitative analysis of effects of compounds **8**, **12**, **16**, and **20–22** on dimensional (A: percent area covered by HUVECs; B: total length per field) and topological parameters (C: numbers of meshes per field; D: numbers of branching points per field) of HUVEC meshwork. Cells were treated with 50 ng/mL FGF-2 with or without 2-PPyQs at highest concentration not inducing decrease in cell viability. Data are expressed as percent change from control value and bars are means \pm SD of four separate experiments; * p < 0.05 from control or FGF-2-treated cultures, Student's t -test.

5.2.6. Effects on in vivo angiogenesis

The effect of 2-PPyQs on angiogenesis was evaluated using the Matrigel Plug assay. Subcutaneous injection of Matrigel plugs containing 50 ng/mL FGF-2 induced a strong angiogenic response in 4 days, with a 2–4-fold increase in the hemoglobin content compared with plugs containing Matrigel alone (see images in [Supple-](#)

[mentary data](#)). According with the in vitro results, compounds **12**, **16**, **20**, and **22** showed also in vivo a strong anti-angiogenic activity ([Fig. 8](#)). Indeed, like vinblastine, a marked reduction of FGF-2-induced angiogenic response was observed in the plugs containing 0.01 μ M tested compounds.

6. Discussion

Herein we describe studies undertaken to evaluate the effects of some antimicrotubule pyrroloazaflavones on both in vitro and in vivo angiogenesis. The in vitro assays were carried out on HUVECs, considering the growth inhibitory activity, the pro-apoptotic effects, the cell migration inhibition, and the effects on morphogenesis. The in vivo effect was evaluated by means of Matrigel plug assay in C57/BL6 mice. Vinblastine was taken as reference, a well known clinically used chemotherapeutic belonging to microtubule-depolymerising vinca alkaloid family. It was described as vascular disrupting agent and showed to exhibit anti-angiogenic activity at very low concentration with suppression of EC migration and capillary-like structures formation.¹¹ Our results showed that pyrroloazaflavones exert, albeit to different extents, anti-angiogenic activity affecting the various step of the process that leads to the formation of new blood vessels.

Angiogenesis is characterized by EC activation leading to EC proliferation as well as EC migration and capillary-like tube formation.

Growth inhibition assay revealed that 2-PPyQs **8**, **12**, **16**, **20–22** had inhibitory effects on both basal and FGF-2-induced cell proliferation. The ability of these compounds to inhibit EC growth

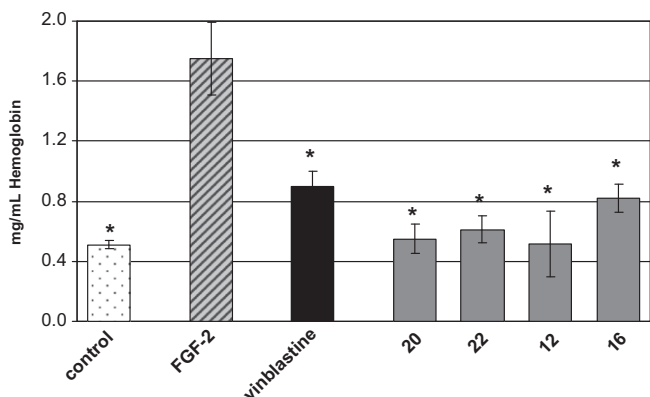


Figure 8. The effect of **12**, **16**, **22**, and **20** treatment on the hemoglobin content in Matrigel plugs. 200 ng/plug FGF-2 and 0.01 μ M tested compounds were injected subcutaneously on dorsal area of C57/BL6 mice. After 7 days, hemoglobin concentration in the plugs was determined. Data are expressed as mg/mL hemoglobin and bars are means \pm SD of three animals; * p < 0.05 from plugs containing only FGF-2, Student's t -test.

in the presence of the growth factor, which is reported to have a role in the development of various tumors, prompted us to investigate the mode by which they induced reduction of the cell number.

Our data indicate that 2-PPyQs have pro-apoptotic activity which is likely to contribute to their anti-angiogenic effects. Several anti-angiogenic agents such as angiostatin and endostatin have been reported to inhibit angiogenesis in part by inducing endothelial cell apoptosis.¹² Moreover, these results match evidence that almost microtubule-affecting agents promote apoptosis in tumor cell lines.^{4,13} Nevertheless, the positive effect of pyrroloazaflavones on apoptosis requires more investigations to assess the mechanism of their cytotoxicity.

The 2-PPyQ derivatives, as vinblastine, have shown to inhibit EC migration, proving an anti-angiogenic activity and at not cytotoxic concentrations. This was further supported by finding that 2-PPyQs prevented capillary-like structure formation in vitro. Addition of 2-PPyQs, at the time of HUVEC seeding on Matrigel, blocked the ability of ECs to align, preventing the formation of tubular structures. Compounds **16** and **22**, due to their remarkable effects on dimensional and topological parameters, greater than those of vinblastine ones, turn out very attractive for further investigations. The inhibitory effect of certain compounds on morphogenesis and cell migration was probably due to their interaction with microtubules, which are involved not only in the formation of the mitotic spindle during cell division, but also play an important role during cell movements.¹⁴ Interestingly, these effects were observed with here 2-PPyQs using in vitro experimental conditions that did not affect cell proliferation. Previously, immunofluorescence assays evidenced that the here **20**, **21** and the 7-methyl-PPyQ were able to destabilize microtubules in Ovar-3 and MCF-7 cell lines, causing loss of the normal microtubule network likewise to that induced by Vincristine: the microtubule network appeared to be 'rarefied' and fragmented.⁶

Our data suggest that the impairment of cytoskeleton fibers could also act together with other mechanism, such as an inhibitory effect on pro-angiogenic factors produced by both endothelial and tumor cells. Indeed, 2-PPyQs inhibited the stimulatory effects induced by FGF-2 on both in vitro cell proliferation and morphogenesis, and in vivo in Matrigel plugs.

Therefore, overall these preliminary studies suggest that 2-PPyQs, although with different profiles, possess anti-angiogenic properties in vitro as well as in vivo. Since these properties were noted under experimental conditions that did not affect EC proliferation, 2-PPyQs might conceivably affect tumor-induced angiogenesis in vivo at local concentration lower than those necessary to cause a cytotoxic effect on tumor cells. Such performance was

already shown for taxanes and cholicidine derivatives as well as for others microtubule/tubulin agents.^{15–20}

7. Conclusions

Collectively, our results clearly indicate that the tested pyrroloazaflavone derivatives bearing the phenyl group at the 2-position, at non-cytotoxic concentrations and like vinblastine, are able (i) to exert in vitro anti-angiogenic activity and (ii) to counteract in vitro and in vivo the pro-angiogenic effects of FGF-2, a well-known cytokine involved in tumor growth. In view of these preliminary results, we are planning further in vivo and in vitro experiments to evaluate whether the here described pyrroloazaflavones could effectively inhibit tumor formation and deeply identify their specific mechanism and molecular targets.

Supplementary data

Supplementary data associated with this article can be found, in the online version, at [doi:10.1016/j.bmc.2010.11.010](https://doi.org/10.1016/j.bmc.2010.11.010).

References and notes

1. Donate, F. *Drugs Future* **2005**, 30, 695.
2. Siemann, D. W.; Bibby, M. C.; Dark, G. G.; Dicker, A. P.; Esken, F. A. L. M.; Horsman, M. R.; Maermè, D.; LoRusso, P. M. *Clin. Cancer Res.* **2005**, 11, 416.
3. Lippert, J. W. *Bioorg. Med. Chem.* **2007**, 15, 605.
4. Mabeta, P.; Pepper, M. S. *Angiogenesis* **2009**, 12, 81.
5. Kanthou, C.; Tozer, G. M. *Int. J. Exp. Pathol.* **2009**, 90, 284.
6. Ferlin, M. G.; Chiarello, G.; Gasparotto, V.; Barzon, L.; Palu', G.; Castagliuolo, I. *J. Med. Chem.* **2005**, 48, 3417.
7. Gasparotto, V.; Castagliuolo, I.; Chiarello, G.; Pezzi, V.; Montanaro, G.; Brun, P.; Palu, G.; Ferlin, M. G. *J. Med. Chem.* **2006**, 49, 1910.
8. Gasparotto, V.; Castagliuolo, I.; Ferlin, M. G. *J. Med. Chem.* **2007**, 50, 5509.
9. Bergman, J.; Sand, P. *Org. Synth.* **1987**, 65, 146.
10. Bergman, J.; Sand, P.; Tilstam, U. *Tetrahedron Lett.* **1983**, 24, 3665.
11. Vacca, A.; Lurlalo, M.; Ribatti, D.; Minischetti, M.; Nico, B.; Ria, R.; Pellegrino, A.; Dammacco, F. *Blood* **1999**, 94, 4143.
12. Folkman, J. *Cancer Biol.* **2003**, 13, 159.
13. Ribatti, D.; Marimipietri, D.; Pastorino, F.; Brignole, C.; Nico, B.; Vacca, A.; Ponzoni, M. *Ann. N.Y. Acad. Sci.* **2004**, 1028, 133.
14. Schwartz, E. L. *Clin. Cancer Res.* **2009**, 15, 2594.
15. Belotti, D.; Vergani, V.; Drudis, T.; Borsotti, P.; Pitelli, R.; Viale, G.; Giavazzi, R.; Tarabozetti, G. *Clin. Cancer Res.* **1996**, 2, 1843.
16. Kanthou, C.; Tozer, G. M. *Blood* **2002**, 99, 2060.
17. Kim, T. J.; Ravoori, M.; Landen, C. N.; Kamat, A. A.; Han, L. Y.; Lu, C.; Lin, Y. G.; Merrit, W. M.; Jennings, N.; Spannuth, W. A.; Langley, R.; Gershenson, D. M.; Coleman, R. L.; Kundra, V.; Sood, A. K. *Cancer Res.* **2007**, 67, 9337.
18. Klauber, N.; Parangi, S.; Flynn, E.; Hamel, E.; D'Amato, R. J. *Cancer Res.* **1997**, 57, 81.
19. Malcontenti-Wilson, C.; Chan, L.; Nikfarian, M.; Muralidharan, V.; Christophy, C. J. *Gastroenterol. Hepatol.* **2008**, 23, c96.
20. Micheletti, G.; Poli, M.; Borsotti, P.; Martinelli, M.; Imberti, B.; Tarabozetti, G.; Giavazzi, R. *Cancer Res.* **2003**, 63, 1534.